Collective Motion of Active Particles and Filaments

Gerhard Gompper

Theoretical Soft Matter and Biophysics
Institute of Complex Systems and Institute for Advanced Simulation
Forschungszentrum Jülich

February 15, 2014

Microswimmers and Self-Propelled Particles

- Many examples:
  bacteria, sperm, paramecium
- Interesting phenomena:
  surface adhesion, vortices,
  metachronal waves

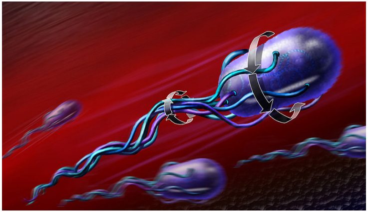

Nicolle Rager Fuller, National Science Foundation

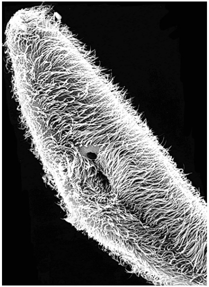

Microswimmers and Self-Propelled Particles

- Many examples:
  bacteria, sperm, paramecium
- Interesting phenomena:
  surface adhesion, vortices, metachronal waves

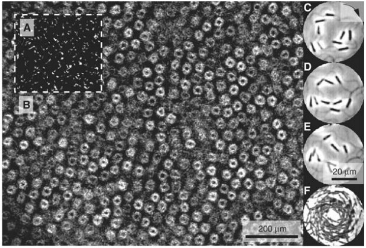

Riedel et al., Science **309**, 300 (2005)

Kaupp et al.

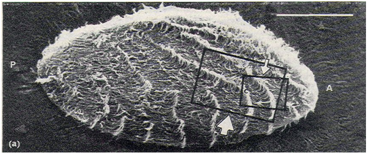

Machemer, Cilia and Flagella (1974)

Outline

- Self-Propelled Rods
- Self-Propelled Spheres
- Curved Flagella

Collective Motion of Self-Propelled Rod-Like Particles

Collective Behavior in Motility Assays

Actin filaments on a carpet of propelling molecular motors

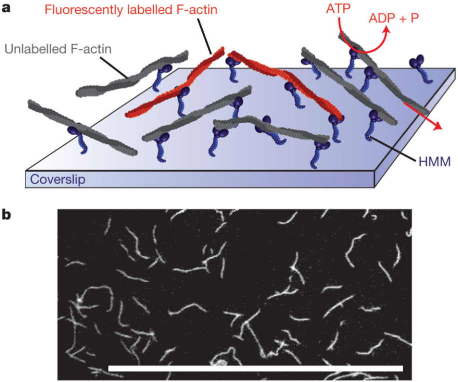

Density waves:

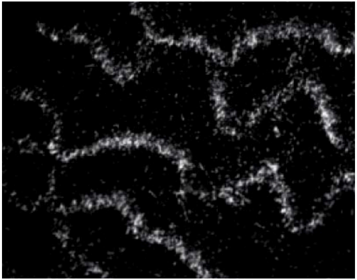

V. Schaller, C. Weber, C. Semmrich, E. Frey, and A. R. Bausch, Nature **467**, 73 (2010)

Penetrable Rod Model in 2D

Forces:

1. Intrinsic swimming force (F_{rod})
2. Noise ($k_{\mathrm{B}}T$)
3. Soft repulsion between rods

   ↪ segment-wise via a separation-shifted Lennard-Jones (SSLJ) potential: energy barrier (E)

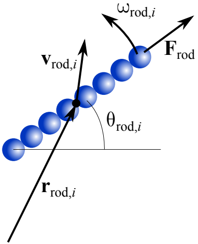

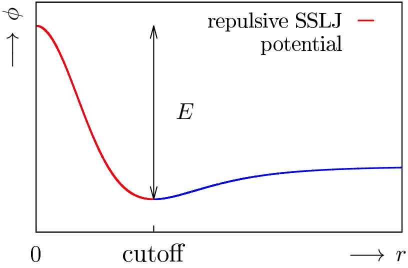

M. Abkenar, K. Marx, T. Auth, G. Gompper, Phys. Rev. E **88**, 062314 (2013)

Penetrable Rod Model in 2D

Forces:

1. Intrinsic swimming force ($F_{\rm rod}$)
2. Noise ($k_{\rm B}T$)
3. Soft repulsion between rods: energy barrier (E)

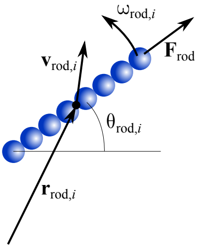

Dimensionless parameters:

- The Péclet number: $Pe = \frac{L_{\rm rod} F_{\rm rod}}{k_{\rm B} T}$
- Penetrability coefficient: $Q = \frac{L_{\rm rod} F_{\rm rod}}{E}$

Penetrating rods $\longrightarrow$ quasi-2D systems

M. Abkenar, K. Marx, T. Auth, G. Gompper, Phys. Rev. E **88**, 062314 (2013)

Rod Crossing Probability

Crossing probability $P(\phi)$ versus collision angle ϕ

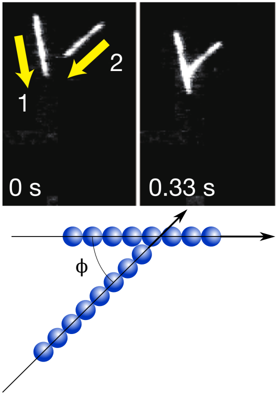

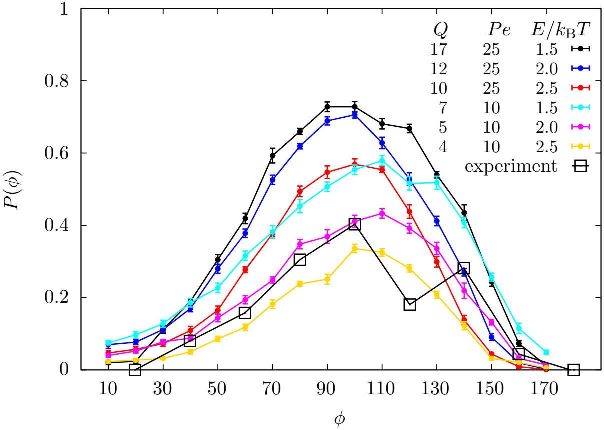

- Highest crossing probability near $\phi \simeq 90°$
- Function shape consistent with experiments with micro-tubules

Y. Sumino *et. al.*, Nature **483**, 448 (2012)

Cluster Break-Up Phase

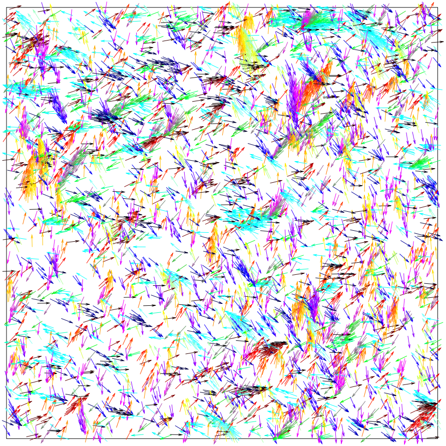

High penetrability Q:

- Single rods and small clusters pass through each-other
- When $F_{\mathrm{swim}} > F_{\mathrm{repulsion}}$

- There is a critical Q for cluster break-up

$Q = 67, \quad Pe = 100, \quad \rho L_{\mathrm{rod}}^2 = 5.1$

Giant Cluster Phase

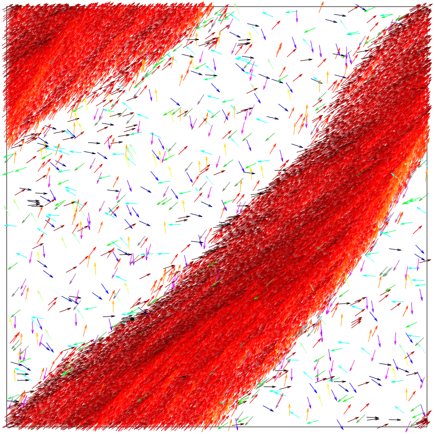

Low penetrability Q:

- Rods collide and align
- A gas of rods around the cluster, density $\rho_{\rm gas}$
- A rate equation gives $\rho_{\rm gas} = (192/\pi^2)(1/L_{\rm rod}^2 Pe)$

- Gas density independent of total density $\longrightarrow$ A vapor density for rods!

$Q = 17, \quad Pe = 25, \quad \rho L_{\rm rod}^2 = 10.2$

Gas Density: Clustering Window

Giant clusters form at high enough *Pe* and low enough *Q*

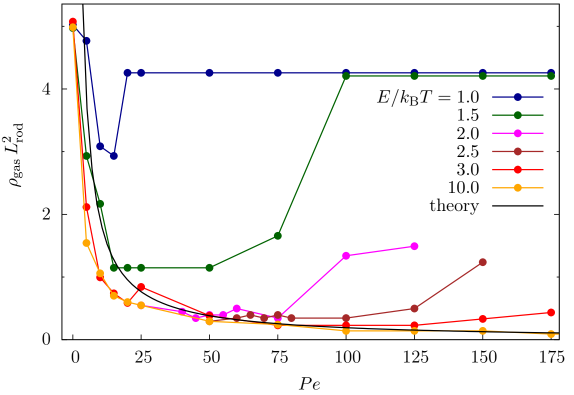

- Low gas density: larger clusters
- ρ_{gas} decreases, and then increases back
- $Pe = \frac{L_{\mathrm{rod}} F_{\mathrm{rod}}}{k_{\mathrm{B}} T}$, $Q = \frac{L_{\mathrm{rod}} F_{\mathrm{rod}}}{E}$

- There is a "clustering window" in propulsion strength
- At low *E*, noise also plays role in cluster break-up

Gas Density: Clustering Window

Giant clusters form at high enough *Pe* and low enough *Q*

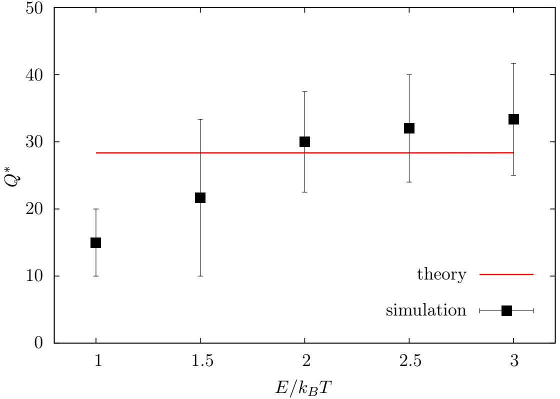

- Low gas density: larger clusters
- ρ_{gas} decreases, and then increases back
- $Pe = \frac{L_{\text{rod}} F_{\text{rod}}}{k_B T}$, $Q = \frac{L_{\text{rod}} F_{\text{rod}}}{E}$

- There is a "clustering window" in propulsion strength
- At low E, noise also plays role in cluster break-up

Cluster Properties

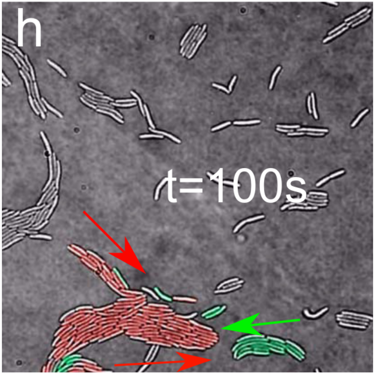

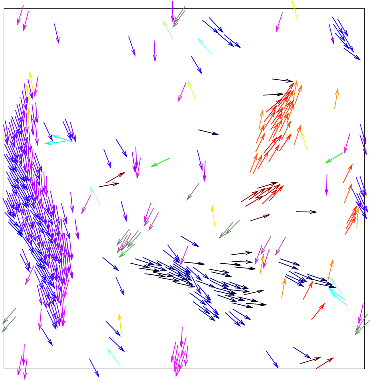

- Polar clusters result from alignment interaction
- Cluster polarity and geometry similar to experiments with myxobacteria

Harvey *et. al.*, New Journal of Physics **15** (2013) 035029

Cluster Size Distributions

Power-law decay in cluster size distributions

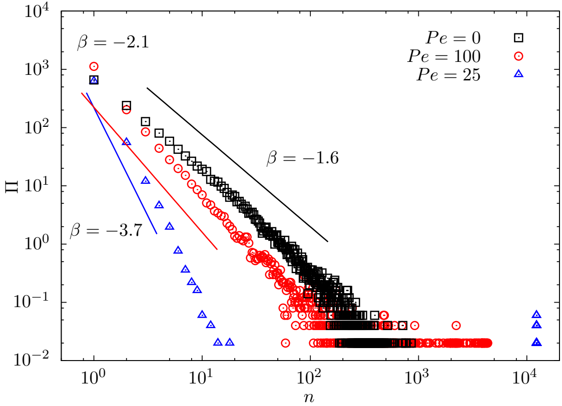

- $\Pi(n) \propto n^{\beta}$
- We obtain $-3.7 < \beta < -1.5$
- Exponents consistent with simulations of hard rods and experiments with myxobacteria

M. Abkenar, K. Marx, T. Auth, G. Gompper, Phys. Rev. E **88**, 062314 (2013)

Y. Yang, V. Marceau, and G. Gompper, *Phys. Rev. E* **82**, 031904 (2010)

F. Peruani *et. al.*, *Phys. Rev. Lett.* **108**, 098102 (2012)

Laning Phase

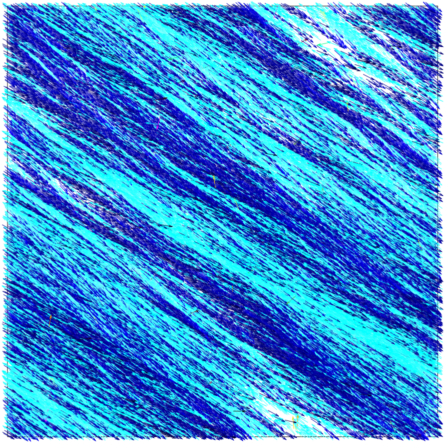

$Q = 67, \quad Pe = 100, \quad \rho\, L_{\mathrm{rod}}^2 = 25.5$

- Very high density
- Streams of rods swimming in opposite directions

Phase Diagram of Self-Propelled Rods

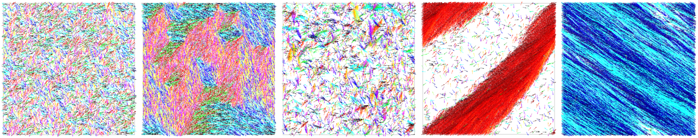

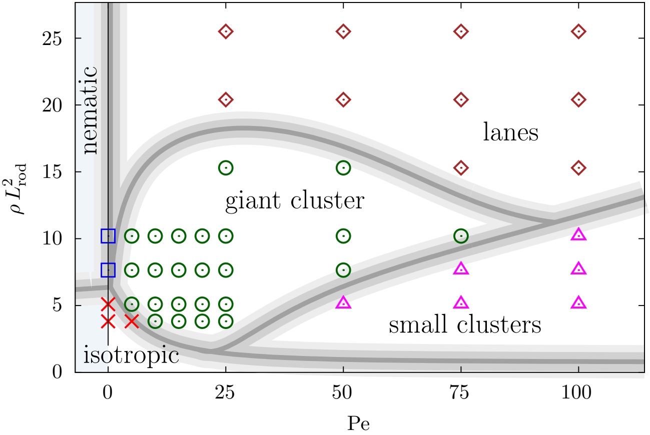

Aggregation and Collective Dynamics

of Self-Propelled Brownian Spheres

Self-Propelled Spheres at Surfaces

Self-propelled Janus colloids (diffusiophoretic, thermophoretic)

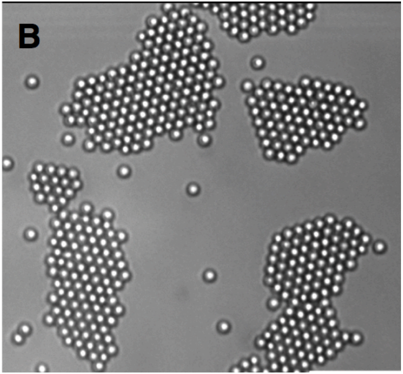

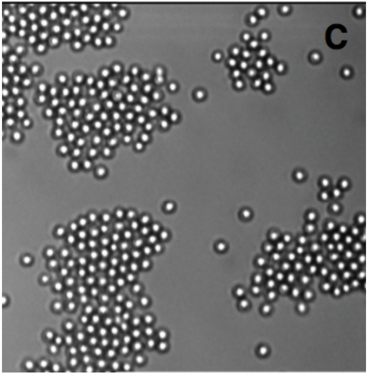

with propulsion

→ crystalline clusters

propulsion switched off

J. Palacci, S. Sacanna, A.P. Steinberg, D.J. Pine, and P.M. Chaikin, Science **339**, 936 (2013).

Brownian Spheres in 3D: Aggregation

Brownian spheres in three dimensions:

- No alignment mechanism – orientational diffusion
- At sufficiently high volume fraction and Pe: phase separation
- Dense phase is fluid
- Droplets → bicontinuous → gas bubbles

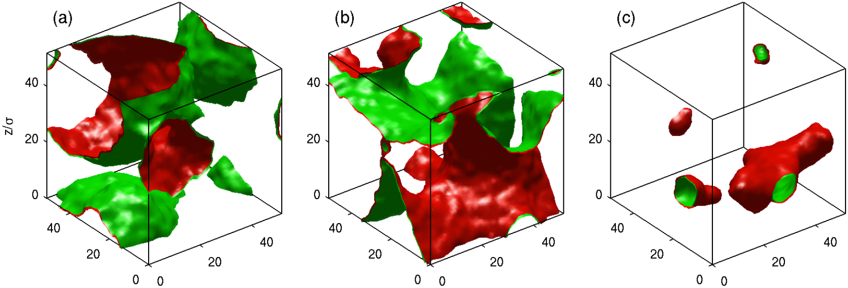

A. Wysocki, R.G. Winkler, G. Gompper, arXiv:1308.6423 (2013)

Brownian Spheres: Domain Geometry (Pe=270)

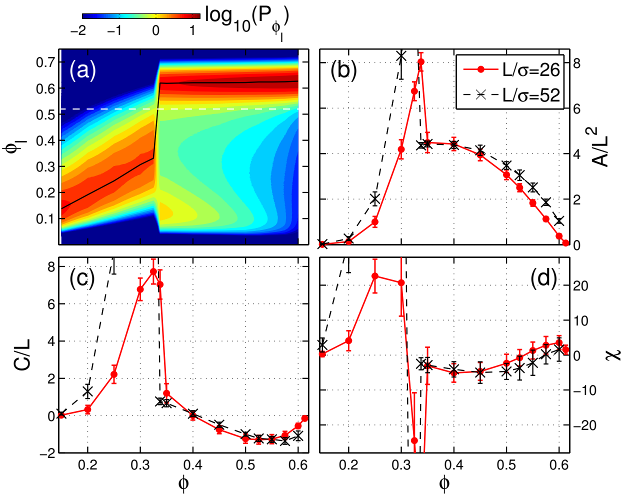

- Note high density of fluid phase $\phi = 0.62$, larger than (passive) glass transition!

Brownian Spheres: Collective Motion (Pe=270)

Collective motion of self-propelled particles without aligning interactions

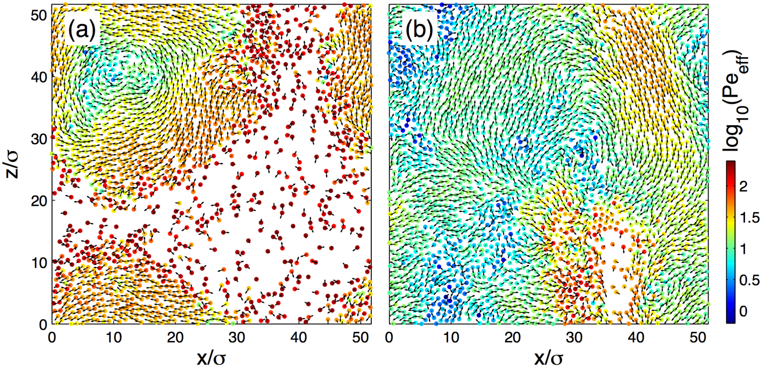

- Swirls and jets due to particle sorting

A. Wysocki, R.G. Winkler, G. Gompper, arXiv:1308.6423 (2013)

Consider single self-propelled Brownian sphere between hard walls

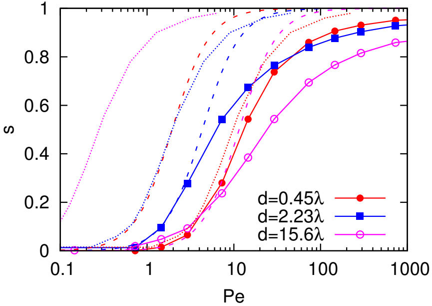

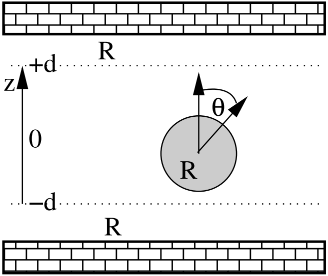

- Sphere shows strong surface adhesion

J. Elgeti & G. Gompper, EPL **101**, 48003 (2013)

Intermezzo: Self-propelled Brownian Sphere between Walls

Solution of Fokker-Planck equation for small Peclet numbers:

$$\begin{aligned}\frac{\rho(z,\theta)}{\rho_0} &= 1 - \frac{Pe}{\sqrt{2}}\exp(-\sqrt{2}z/\lambda)Y_1^0(\theta)\\ &+ \frac{Pe^2}{6}\left[\sqrt{3}\exp(-\sqrt{6}z/\lambda) - \exp(-\sqrt{2}z/\lambda)\right]Y_2^0(\theta)\\ &+ \frac{Pe^2}{6}\exp(-\sqrt{2}z/\lambda) + \mathcal{O}(Pe^3)\end{aligned}$$

Surface excess:

$$s = \frac{\lambda Pe^2}{6\sqrt{2}} + \mathcal{O}(Pe^4)$$

J. Elgeti & G. Gompper, EPL **101**, 48003 (2013)

Compare with simulation results

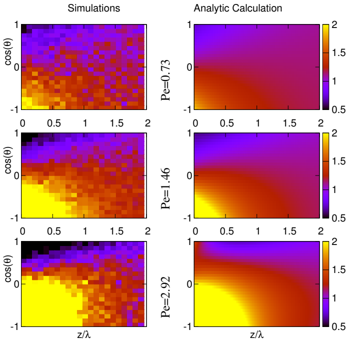

Brownian Spheres: Collective Motion

Displacement pair correlation function

$$C_d(r, \Delta t) = \frac{\left\langle \sum_{i,j\neq i} \mathbf{d}_i \cdot \mathbf{d}_j \, \delta(r - |\mathbf{r}_i - \mathbf{r}_j|) \right\rangle_t}{c_0 \left\langle \sum_{i,j\neq i} \delta(r - |\mathbf{r}_i - \mathbf{r}_j|) \right\rangle_t},$$

depends on time lag Δt via displacement vector $\mathbf{d}_i = \mathbf{r}_i(t + \Delta t) - \mathbf{r}_i(t)$.

Global measure of cooperativity

$$\chi_d(\Delta t) = \int_\sigma^{L/2} C_d(r, \Delta t) \, \mathrm{d}^3 r.$$

Brownian Spheres: Collective Motion (Pe=270)

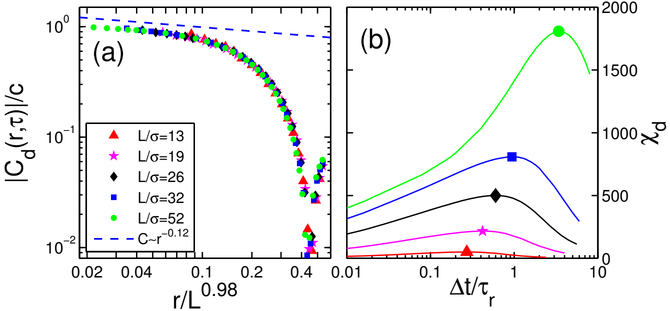

- Correlations very long ranged
- Build-up time τ required to reach maximum cooperativity!
- Correlation time τ strongly depends on system size.

A. Wysocki, R.G. Winkler, G. Gompper, arXiv:1308.6423 (2013)

Brownian Spheres: Propulsion vs. Noise

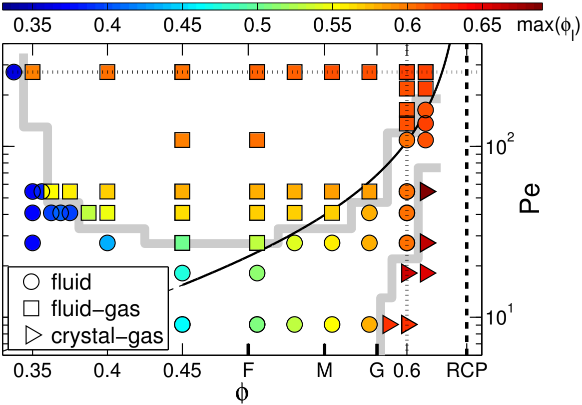

- Minimum Peclet number $Pe_c \simeq 30$ required to generate phase separation!

A. Wysocki, R.G. Winkler, G. Gompper, arXiv:1308.6423 (2013)

Flagellar Vortices

Sperm Vortices

Spermatozoa spontaneously form vortices at surfaces at high concentration

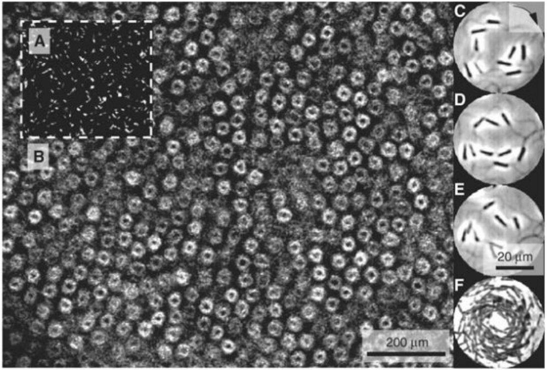

I.H. Riedel, K. Kruse, and J. Howard, Science **309**, 300 (2005)

Single Sperm near Surfaces

Mesoscale hydrodynamics simulations show

- effective attraction of sperm to surfaces
- due to hydrodynamic interactions and elongated shape
- circular motion for chiral sperm shapes

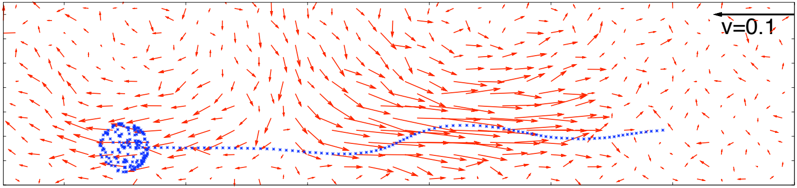

J. Elgeti, U.B. Kaupp, and G. Gompper, Biophys. J. **99**, 1018 (2010)

Single Sperm near Surfaces

Mesoscale hydrodynamics simulations show

- effective attraction of sperm to surfaces
- due to hydrodynamic interactions and elongated shape
- circular motion for chiral sperm shapes

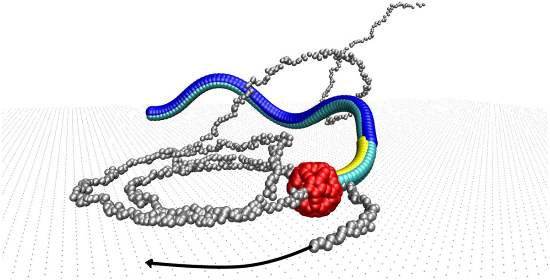

J. Elgeti, U.B. Kaupp, and G. Gompper, Biophys. J. **99**, 1018 (2010)

Dense Flagella Systems in Two Dimensions

Flagellum described as semi-flexible polymer

- chain of beads
- curvature elasticity
- time-dependent spontaneous curvature

$$c(s,t) = A\sin(qs - 2\pi f_0 t)$$

with beat frequency f_0.

(b)

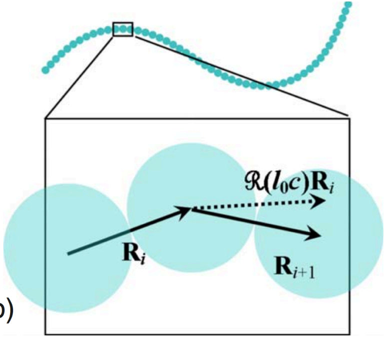

Y. Yang, V. Marceau, and G. Gompper, Phys. Rev. E **82**, 031904 (2013)

Dense Flagella Systems in Two Dimensions

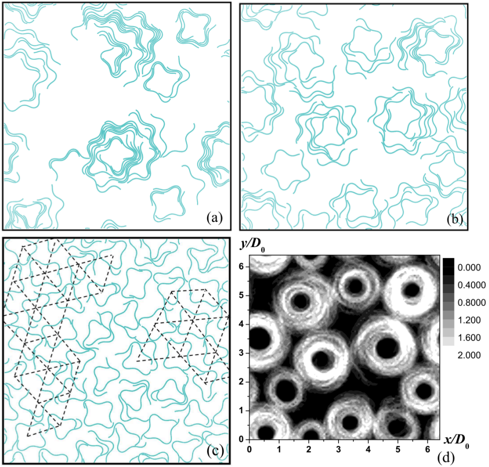

(a) with hydrodynamic interactions
(b) anisotropic friction, small curvature
(c) anisotropic friction, large curvature

(d) same as in (b), averaged over 30 beats.

Y. Yang, F. Qiu, and G. Gompper, Phys. Rev. E **89** 012720 (2014)

Dense Flagella Systems in Two Dimensions

- much stronger correlations without hydrodynamics
- hydrodynamics in 2D over-estimates hydrodynamics near wall in 3D

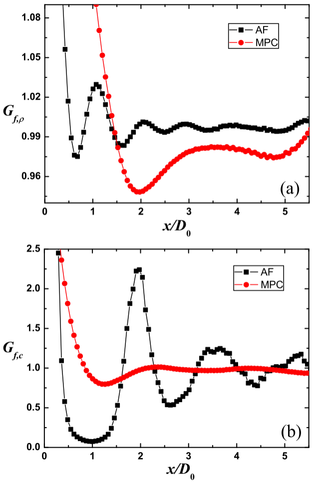

Dense Flagella Systems in Two Dimensions

Order parameter

$$S = \Delta^2/\Delta_0^2 - 1$$

where Δ^2 is variance of trajectory centers in area D_0^2.

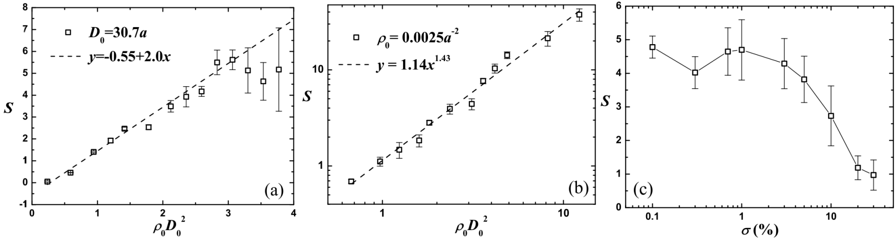

Y. Yang, F. Qiu, and G. Gompper, Phys. Rev. E **89** 012720 (2014)

Comparison with experiment:

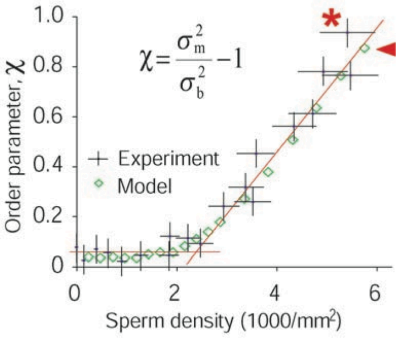

I.H. Riedel, K. Kruse, and J. Howard, Science **309**, 300 (2005)

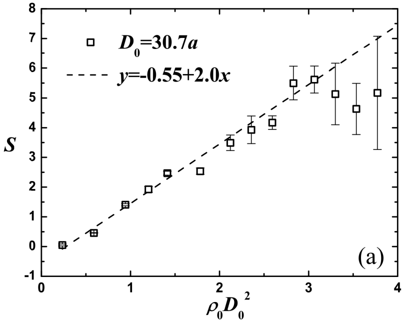

Y. Yang, F. Qiu, and G. Gompper, Phys. Rev. E **89** 012720 (2014)

Summary & Conclusions

- Shape, orientational fluctuations and hydrodynamics together determine dynamics of microswimmers
- Aggregation and clustering generic feature of self-propelled particles
- Penetrable self-propelled rods – motile clusters and laning
- Brownian spheres – phase separation and collective dynamics
- Sperm dynamics – wall adhesion and circular motion
- Multiple sperm dynamics – vortex formation

Masoud Abkenar

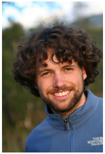

Jens Elgeti

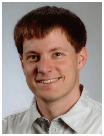

Thorsten Auth

Adam Wysocki

Yingzi Yang

Roland Winkler